“To spin or not to spin?” -Is spin-coating the ideal technique for pre-deposition of sodium fluoride for CIGS rear surface passivated ultrathin solar cells?

Gizem Birant[1,2,3,*], Jessica de Wild[1,2,3], Marc Meuris[1,2,3], Jef Poortmans[3,4,5], and Bart Vermang[1,2,3]

1 Institute for Material Research (IMO), Hasselt University (partner in Solliance), Wetenschapspark 1, 3590 Diepenbeek, Belgium.
2 imec division IMOMEC (partner in Solliance), Wetenschapspark 1, 3590 Diepenbeek, Belgium.
3 EnergyVille, Thorpark, Poort Genk 8310 & 8320, 3600, Belgium
4 imec (partner in Solliance), Kapeldreef 75, Leuven, 3001, Belgium.
5 Department of Electrical Engineering, KU Leuven, Kasteelpark Arenberg 10, 3001, Heverlee, Belgium
Correspondence: gizem.birant@imec.be

Introduction

To pursue the aim for cleaner energy, photovoltaics reveals itself as one of the best possible options. Although silicon-based (Si) solar cells act as the sector leader due to their technology readiness, thin-film solar cells have advantages like being able to deposit on flexible surfaces, tunable bandgap, and transparency. Among various thin-film technologies, CIGS is one of the best efficient thin-film technologies [1]. Even though CIGS has superior efficiency among other thin-film technologies, it is still behind the theoretical efficiency limit [2]. Furthermore, in order to make the CIGS solar cells more industrially viable, one way is to reduce the thickness of the absorber layer. However, reducing the thickness of the active layer of the solar cell results in insufficient absorption and detrimental impacts of back surface recombination [3]. To overcome this problem, adding a passivation layer with point contact openings is a proven approach [3][4][5]. After depositing the passivation layer, our previous works studied a novel approach, named alkali salt selenization, to create the contact openings in the passivation layer [6],[7],[8]. We chose spin coating to deposit the alkali salt on the dielectric layer due to its easiness, cost-effectiveness, and the possibility to convert a more industrially viable approach like spray pyrolysis or ultrasonic spray deposition. However, via spin-coating, there is a possibility that the layer is deposited unevenly, and salt particles can unwantedly accumulate and create clusters. This study will share the optical and electrical characterizations of a single solar cell sample with the optimal and non-optimal amounts of sodium fluoride (NaF), which is the result of the spin-coating process. Furthermore, we will share our insights about the question we asked in our title, to spin or not to spin the NaF on the passivation layers.

Methodology

Production of the rear-passivated solar cells: The passivation layer, 6nm thick AlOx, is atomic-layer-deposited (ALD) on soda-lime glass/Mo substrate, which has ~100nm Si(O, N) alkali barrier layer at 300°C. Trimethylaluminum (TMA) was used as the precursor, and H2O was used as the reactant during the deposition. The nm/cycle rate was calculated to be 0.17 by assuming a constant growth rate with time. The alkali solution, 0.4M NaF, spin-coated on the dielectric layer with 3000rpm. The 500nm thick CIGS layer is grown via single-stage co-evaporating technique with CGI ([Cu]/([In]+[Ga])) of ~0.8, and GGI ([Ga]/([In]+[Ga])) of ~0.3, measured with XRF. The solar cells are finished with chemical bath deposition of CdS

buffer layer and evaporation of ZnO and ITO layers as window layers. The metal silver (Ag) grids are also evaporated, more detailed explanation can be found elsewhere [9].

Measurement setups:

Solar cell measurement: The solar cell (6 cell in total, 3 with optimal and 3 with non-optimal NaF) is measured under AM 1.5 spectra via Keithley 2400 source meter with 4-point probe. The solar cell parameters are derived from the JV curve under light illumination via MATLAB routine with 1-diode model.
Hyperspectral imaging: A global hyperspectral imager is used for hyperspectral imaging. (Photon etc., Canada) In order to homogenously excite the sample, 532nm laser is used, and the optical and photoluminescence (PL) images are taken via InGaAs camera with 800mW intensity, 3nm spectral and 2.2 µm lateral resolution. The reflection data is normalized over the lamp spectrum.
Scanning electron microscopy (SEM) imaging: SEM imaging is realized with a Tescan and Bruker SEM. A 15kV accelerating voltage is used with different magnifications.

Results and discussions

Solar cell results:

The sketch and the actual photo of the measured solar cell are shared in Figure 1. Due to an experimental error during spin coating, the right side of the sample was not coated optimally with NaF. As can be seen from the photo of the solar cell, the right part has a darker shade, i.e., less NaF compared to the left side.

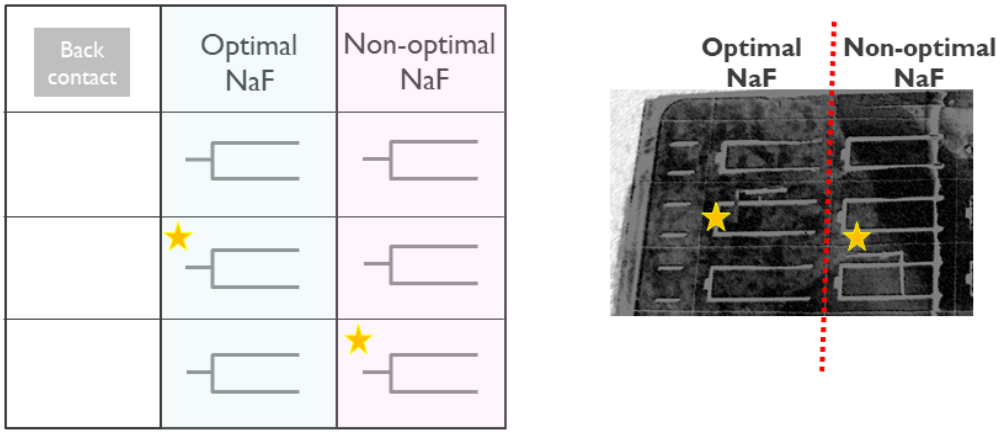

Figure 1 The sketch and the actual photo of the tested solar cell. The left part (green part) of the solar cell has an optimal amount of NaF while the right part (pink part) has non-optimal due to spin-coating failure. The stars represent the cell that hyperspectral imaging is realized.

The solar cell results reveal the difference between the two sides of the solar cell, and the part with an optimal NaF amount has superior results than the part with non-optimal NaF amount. (Figure 2) As can be seen from Fig.2-a, in between two parts of the same solar cell, there has been a 42% drop in short-circuit current (Jsc), a 13% drop in open-circuit voltage (Voc), a 61% drop in fill factor (FF), and hence a 79% drop in efficiency values.

The illuminated JV curve for a non-optimal amount of NaF shows the reason for dropped solar cell parameters. There is an apparent kink in the curve. There are two possible reasons for this

kink; the first is the lack of sodium. The second is the lack of contact openings in the passivation layer, which is again the result of not having enough sodium on the layer to create the openings, for details kindly refer to [6].

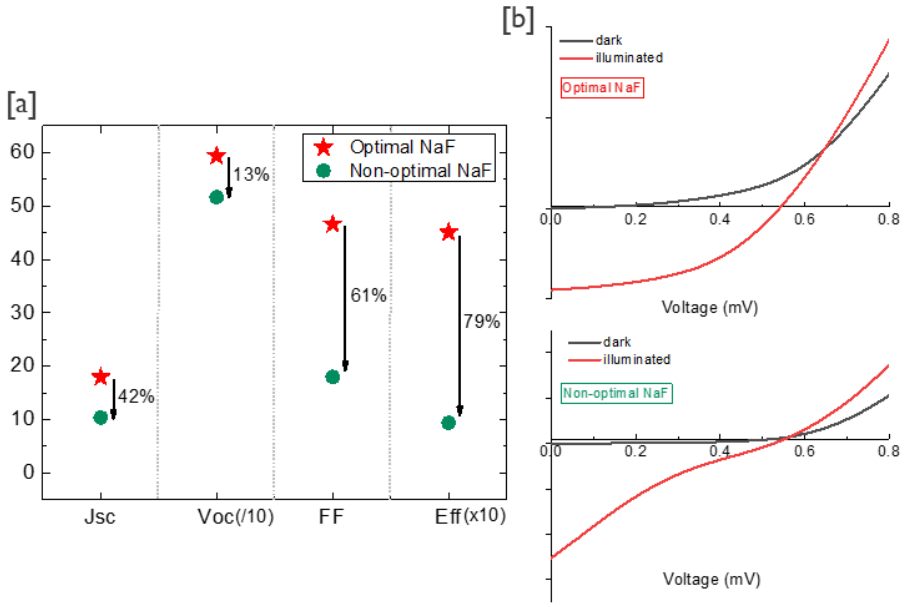

Figure 2 a- Solar cell parameters for optimal (represents with a red star) and non-optimal (represents with a green dot) amount of NaF, and **b-** dark (black line) and illuminated (red line) JV curves of solar cells with optimal (up) and non-optimal (down) amount of NaF. *The Voc values are divided by 10, and the efficiency values are multiplied by 10 for better visualization.*

Hyperspectral imaging (mapping):

In order to see the effect of the sodium on PL yield, hyperspectral imaging is realized for two cells. The PL and reflection are laterally measured with hyperspectral imaging. Figure 3 represents the PL mapping (a and b) and PL yield (c and d) for two sides of the solar cell, with the comparison of PL yields (e) for both sides. The measurement was realized for the cells marked with a star in the sketch shared in Fig.1.

Every pixel of the map with high and low intensities, i.e., a shiny and a dark dot, gives a PL and reflection spectra at a specific wavelength. Looking at the PL mapping for two sides of the solar cell, there is a visible difference in between these two maps that the shiny dots in the left map (Fig.3-a) is smaller and less populated than the ones in the right map (Fig.3-b). The reason will be explained in detailed in the following paragraphs.

The PL yields also reveal the difference between the two sides, Fig.3 c and d. The maximum intensity reached from the left side of the sample, i.e., less (non-optimal) Na amount, is almost equal to the minimum response reached from the right side of the sample, i.e., optimal Na amount. This difference may also explain the difference in the Voc values of the solar cells since higher intensity means less non-radiative recombination. For a more precise comparison, the total area PL intensities are shared inside the same graph in Fig.3-e. The difference in the PL intensity peaks is more obvious in this graph. Also, for the side with less Na has a broader peak in the long-wavelength region as expected, the reason is explained somewhere else [10].

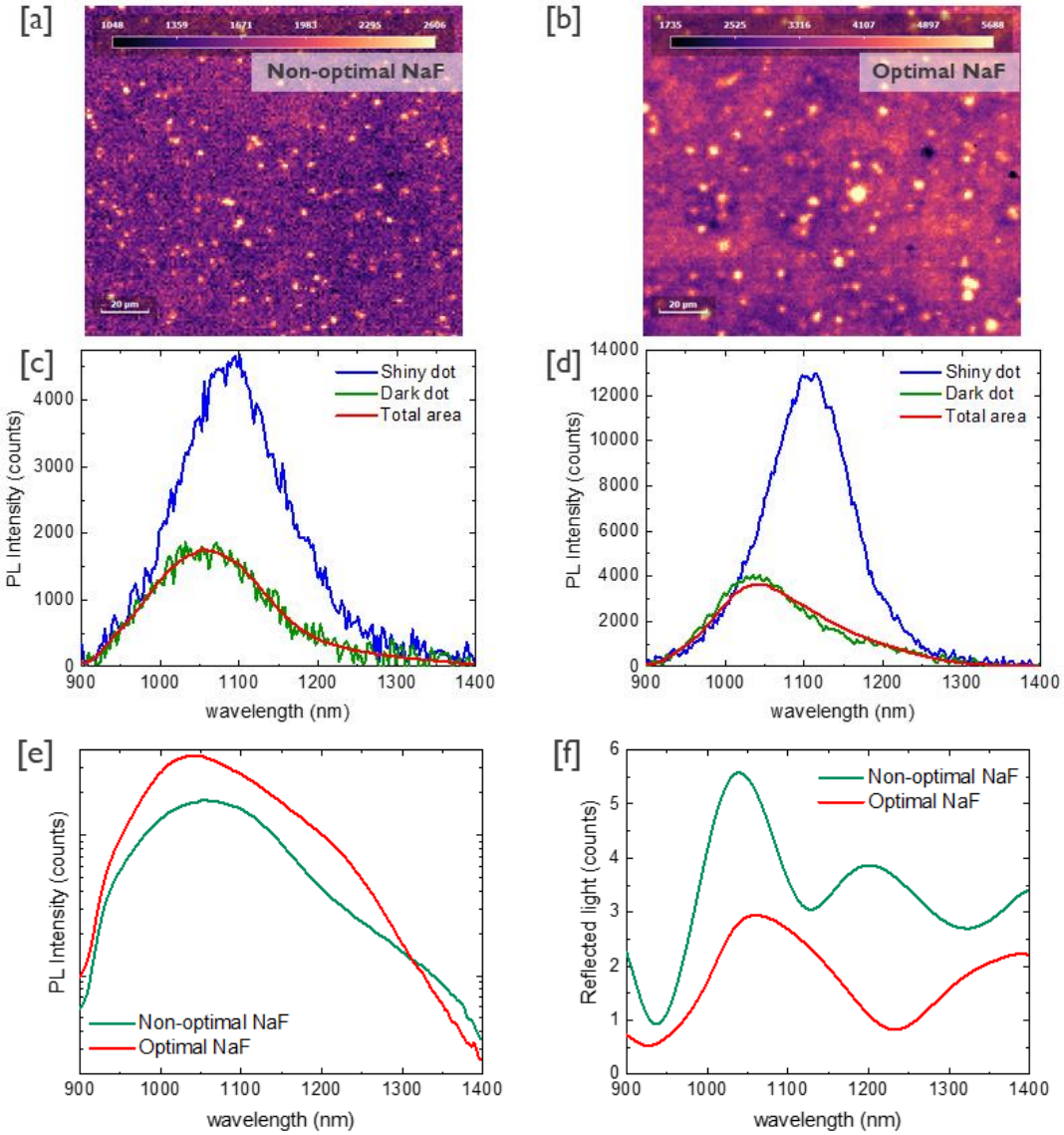

Figure 3 The PL mapping of the solar cell with **a**-non-optimal amount and **b**-optimal amount of NaF, with 20µm magnification. The PL yield of the solar cell from a shiny dot, dark dot, and total area of the solar cell with **c**-non-optimal and **d**-optimal amount of NaF. The comparison of **e**- PL yields and **f**- reflected light of total areas for two sides of the solar cell.

Spin-coating- pros and cons:

Until so far, we discussed the difference in optimal and non-optimal Na amounts and their effects on the electrical and optical characteristics of the solar cell. Now, we will further investigate the spin-coating mechanism and its usefulness in our approach. Spin-coating is a methodology that uses centrifugal force to apply a uniform film onto a solid surface. The centrifugal force of the rotation spreads the liquid into a film and covers the substrate [11]. In our process, a liquid, i.e., alkali solution, is placed onto the substrate to cover the whole surface. Then the substrate is rapidly rotating to produce a uniform layer. However, this approach is open to error due to the operator because the duration of the process depends on the color change on the surface, and hence by a personal judgment. The idea behind the color change is the spin-coated film absorbs and reflects the light in different wavelengths resulting in a color change during the process [12]. Once, uniform color has reached, the process is stopped manually. Furthermore, the amount of solution applied onto the substrate is not precisely the

same in every attempt; hence the amount of Na onto the substrates is different from sample to sample even the aim is to deposit the same amount. As a result, the Na layer onto our substrate is not homogenous as can be seen from Figure 4.

The SEM images of the spin-coated Na onto our substrate can be seen from Fig.4 a and b. In Fig.4 a, the inhomogeneity of the salt layer, and in Fig.4 b, the difference in the size of the salt particles and accumulations are visible. The hyperspectral PL mapping of the sample with optimal Na amount is also shared in Fig.4, c and d, the far-view and the close-up, respectively. The high-intensity parts, i.e., yellow parts, are the Na particles, which supports the SEM images in terms of inhomogeneity and size difference. This difference is also visible in the PL maps that are shared in Fig.3 a and b, that one side of the sample has less Na than the other side of the sample. Hence, the brighter response corresponds to higher amounts of Na (Fig.3 a and b).

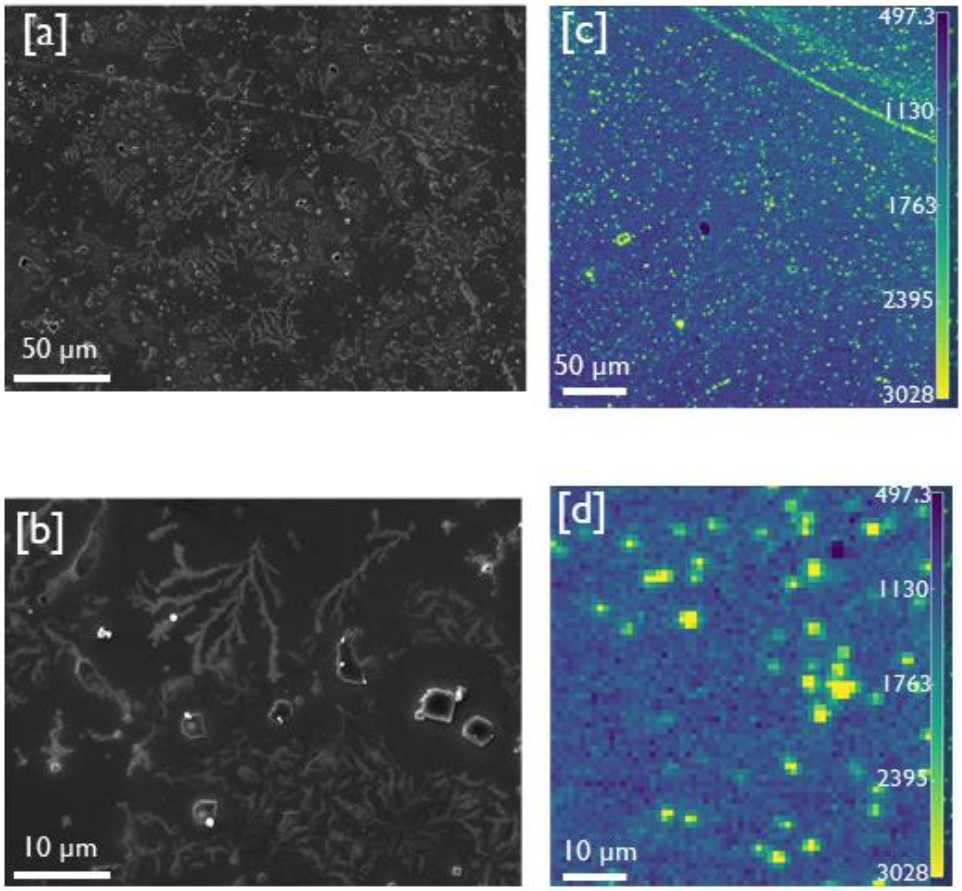

Figure 4 Scanning electron microscopy (SEM) images of the sample with optimal Na amount with **a**-1000x and **b**-5000x magnifications. (*Light grey shapes are the salt particles and thinner salt layer, i.e., branches*) PL mapping of the same sample **c**- far-view and **d**-close-up distance. (*Higher intensity shapes (luminescent yellow) are Na salt particles*.)

The inhomogeneous distribution of the Na particles affects also solar cell performance. The Na tends to hold onto the AlOx rear passivation layer [13]. Hence, the diffusion of the Na amount into the absorber layer differs, effects the doping level, (Supporting Figure 1) and, resulting in deteriorated solar cell performance. As can be seen from Fig.2, even for optimal Na amount, the Voc values are significantly lower than reported record efficient solar cells. Furthermore,

the inhomogeneous Na layer also affect the contact opening formation as reported in [6]. As a result, the overall performance of the solar cell is not meeting the expectations.

Conclusion

In this study, the effect of Na amount on the solar cell performance is shown with a single solar cell structure. Due to an experimental failure in the spin-coating process, one-half of the sample could not reach the optimal amount of Na. This claim was supported with hyperspectral imaging (mapping), PL, and reflectance measurement. Furthermore, the solar cell performance of this part of the solar cell was severely affected by this failure. Even with an optimal amount of Na, the desired solar cell performance could not reach. The reason for this lower performance is the inhomogeneously distributed Na layer due to spin coating. Since Na tends to attach to the AlOx passivation layer, this inhomogeneous distribution alters the diffusion into the absorber layer, hence the doping level of the solar cell. By simply changing the deposition technique of the Na solution with evaporation or spray pyrolysis, these problems can be solved. Hence, the answer to the question in the title should be "not to spin!"

Acknowledgement

This work received funding from the European Union's H2020 research and innovation program under grant agreement No. 715027.

References

[1] M. A. Green, E. D. Dunlop, J. Hohl-Ebinger, M. Yoshita, N. Kopidakis, and X. Hao, "Solar cell efficiency tables (Version 58)," *Prog. Photovoltaics Res. Appl.*, vol. 29, no. 7, pp. 657–667, Jul. 2021.

[2] W. Shockley and H. J. Queisser, "Detailed Balance Limit of Efficiency of p-n Junction Solar Cells," *J. Appl. Phys.*, vol. 32, no. 3, pp. 510–519, Mar. 1961.

[3] G. Birant, J. de Wild, M. Meuris, J. Poortmans, and B. Vermang, "Dielectric-Based Rear Surface Passivation Approaches for Cu(In,Ga)Se2 Solar Cells—A Review," *Appl. Sci.*, vol. 9, no. 4, p. 677, Feb. 2019.

[4] D. Ledinek, J. Keller, C. Hägglund, W. C. Chen, and M. Edoff, "Effect of NaF pre-cursor on alumina and hafnia rear contact passivation layers in ultra-thin Cu(In,Ga)Se2 solar cells," *Thin Solid Films*, vol. 683, no. November 2018, pp. 156–164, 2019.

[5] B. Vermang, X. Gao, and M. Edoff, "Improved Rear Surface Passivation of Cu(In,Ga)Se2 Solar Cells : A Combination of an Al2O3 Rear Surface Passivation Layer and Nanosized Local Rear Point Contacts," vol. 4, no. 1, pp. 486–492, 2014.

[6] G. Birant *et al.*, "Innovative and industrially viable approach to fabricate AlOx rear passivated ultra-thin Cu(In, Ga)Se2 (CIGS) solar cells," *Sol. Energy*, 2020.

[7] I. Kandybka *et al.*, "Novel cost-effective approach to produce nano-sized contact openings in an aluminum oxide passivation layer up to 30 nm thick for CIGS solar cells," *J. Phys. D. Appl. Phys.*, vol. 54, no. 23, p. 234004, Jun. 2021.

[8] G. Birant *et al.*, "Rear surface passivation of ultra-thin CIGS solar cells using atomic layer deposited HfO x," *EPJ Photovoltaics*, vol. 11, p. 10, Dec. 2020.

[9] J. de Wild *et al.*, "High Voc upon KF Post-Deposition Treatment for Ultrathin Single-Stage Coevaporated Cu(In, Ga)Se2 Solar Cells," *ACS Appl. Energy Mater.*, vol. 2, no. 8, pp. 6102–6111, 2019.

[10] J. De Wild, M. Simor, D. G. Buldu, T. Kohl, G. Brammertz, and M. Meuris, “Alkali treatment for single-stage co-evaporated thin CuIn0.7Ga0.3Se2 solar cells,” *Thin Solid Films*, vol. 671, pp. 44–48, 2019.
[11] R. Smith, H. Inomata, and C. Peters, “Historical Background and Applications,” in *Introduction to Supercritical Fluids*, vol. 4, 2013, pp. 175–273.
[12] Jorge Alexandre de Abreu Mafalda, “Advanced rear contact design for CIGS solar cells,” KTH Royal Institute of Technology, 2019.
[13] J. de Wild *et al.*, “Detrimental Impact of Na Upon Rb Postdeposition Treatments of Cu(In,Ga)Se 2 Absorber Layers,” *Sol. RRL*, p. 2100390, Jul. 2021.

Supplemantary Figure

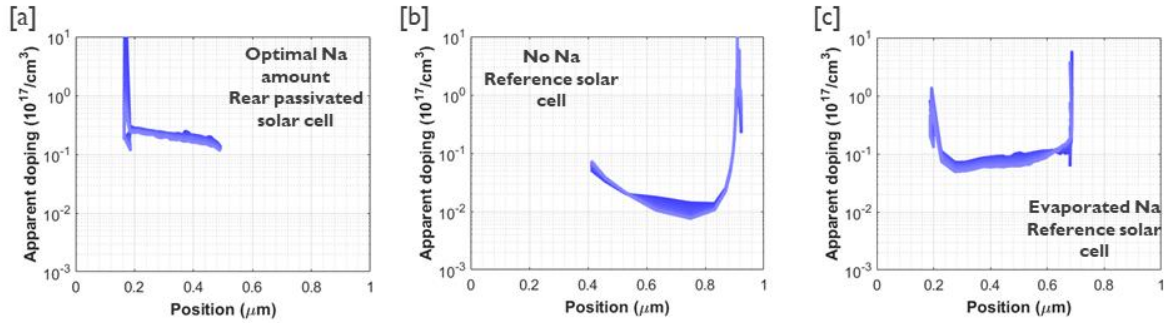

Supplementary Figure 1 The doping levels of solar cells with **a-**optimal amount of Na (rear surface passivated), **b-** without any Na (reference) and **c-**evaporated Na (reference)